IX. COMMUNICATION RESEARCH

A. MULTIPATH TRANSMISSION

Prof. L. B. Arguimbau
E. J. Baghdady
E. E. Manna
O. P. McDuff
R. A. Price
C. K. H. Tsao

1. Transatlantic Tests

Work on the receiver trapping circuits is complete, but investigations of the diversity and waveform-repair circuits are still in progress.

C. K. H. Tsao, E. E. Manna

2. FM Receiver Design

a. Narrow-band limiting

The work of the FM group on interference rejection, as reported in previous Quarterly Progress Reports and by J. Granlund (Interference in Frequency-Modulation Reception, Technical Report No. 42, Research Laboratory of Electronics, M.I.T. 1949), indicates that a good rapid-acting wideband limiter followed by a rapid-acting wideband detector is a sufficient requirement for the complete separation of two signals that have an arbitrarily small difference in magnitude. The question as to whether this is a necessary requirement remains unanswered. In fact, as suggested in Granlund's report, there might be some advantages to be gained from a process of limiting followed by narrow-band filtering before the signal is finally detected. This question is now being investigated both theoretically and experimentally.

E. J. Baghdady

b. Gated-beam limiters

As previously reported (1) 6BN6 tubes make convenient limiters. They have the advantage of drawing relatively low grid currents and depending on plate-current rather than grid-current action. Thus the circuits can be made quick-acting, and the troublesome grid-circuit time constant characteristic of a pentode limiter can be avoided. These tubes have recently been studied further (2). As indicated in the preferred circuit arrangement of Fig. IX-1 the bias on the first (limiter) grid should be somewhat higher than that on the third (quadrature) grid. Figure IX-2 shows a set of limiter characteristics obtained for various limiter-grid biases with the quadrature bias fixed at -1.25 volts. This shows that the optimum bias adjustment is somewhat critical. Figure IX-3 shows the way the effective input impedance varies with the input signal level for various grid biases.

R. A. Price

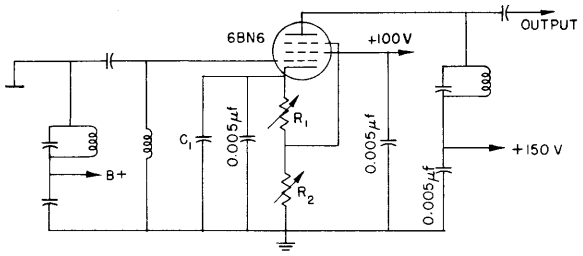

Fig. IX-1
6BN6 limiter circuit.

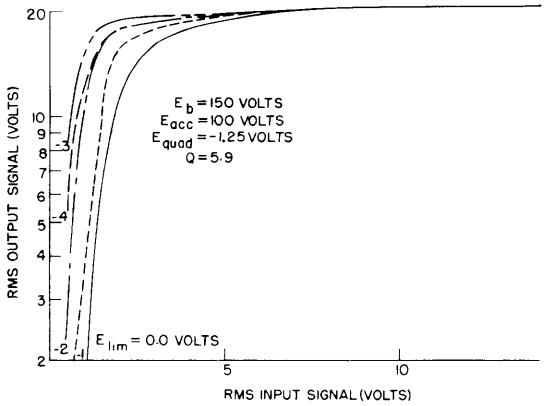

Fig. IX-2
Output signal vs input signal.
Limiter bias varied.

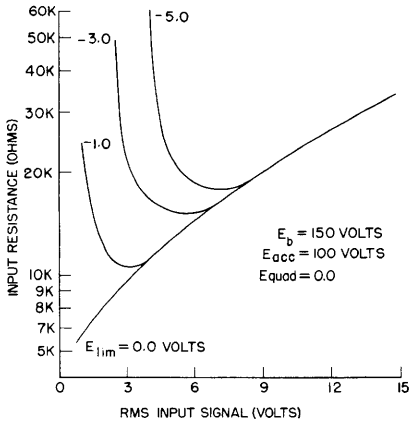

Fig. IX-3
Input resistance vs input signal.

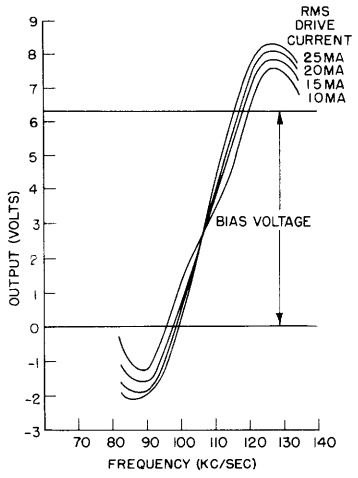

Fig. IX-4
Experimental output curves for 6.3-volt bias.

References

1. Quarterly Progress Report, Research Laboratory of Electronics, M.I.T. Jan. 15, 1952, p. 49
2. R. A. Price: A Study of the Gated Beam Limiter, Master's Thesis, Department of Electrical Engineering, M.I.T. 1953

c. Ratio detection

The operation of a ratio detector using ideal assumptions has previously been discussed by J. Granlund (1). O. P. McDuff (2) has extended this analysis to cover the actual operation with physical diodes.

It is shown that the chief limitation of the simplified analysis is the assumption of diodes conducting in short pulses. A Fourier analysis is applied to the diode currents, and a theoretical study which makes an assumption regarding diode conduction angle is shown. The computed results thus obtained check well with experimental results.

A discussion of the parameters likely to affect the circuit under various operating conditions is included. Experimental and calculated results showing the effects of various parameters are presented.

Typical curves are shown in Fig. IX-4.

L. B. Arguimbau

References

1. J. Granlund: Interference in Frequency-Modulation Reception, Technical Report No. 42, Research Laboratory of Electronics, M.I.T. 1949
2. O. P. McDuff: A Study of a Modified Ratio Detector Operating Under Non-Ideal Conditions, Master's Thesis, Department of Electrical Engineering, M.I.T. 1953

(IX. COMMUNICATION RESEARCH)

B. STATISTICAL THEORY OF COMMUNICATION

Prof. J. B. Wiesner	Prof. J. F. Reintjes	Dr. B. Mandelbrot
Prof. R. M. Fano	P. E. Green, Jr.	Dr. F. A. Muller
Prof. Y. W. Lee	R. M. Lerner	I. Uygur

1. A New Principle for a Pitchfinder

A pitchfinder is an instrument to measure the periodicity of speech signals. It is used for scientific phonetic research and for vocoder systems. Since the instruments used up to now are not quite satisfactory, a pitchfinder based upon a new principle is under construction. The principle is illustrated in Fig. IX-5.

The speech signal is represented by the function f. Let $f(0)$ be the value of f at some arbitrary time $t = 0$. The function f will assume the same value $f(0)$ at a number of times t_1, t_2, and so forth. One of these is equal to the period T of the signal, and our objective is to determine it.

For this purpose we generate a different periodic function ϕ by passing f through some distorting network with a short memory (provided it does not generate subharmonics). Let $\phi(0)$ be the value of ϕ at $t = 0$. The function ϕ will be equal to $\phi(0)$ at the times t_1, t_2, and so forth. One of these will be equal to the period T, which is the same as for the function f. The other times within the first period at which $\phi = \phi(0)$ are

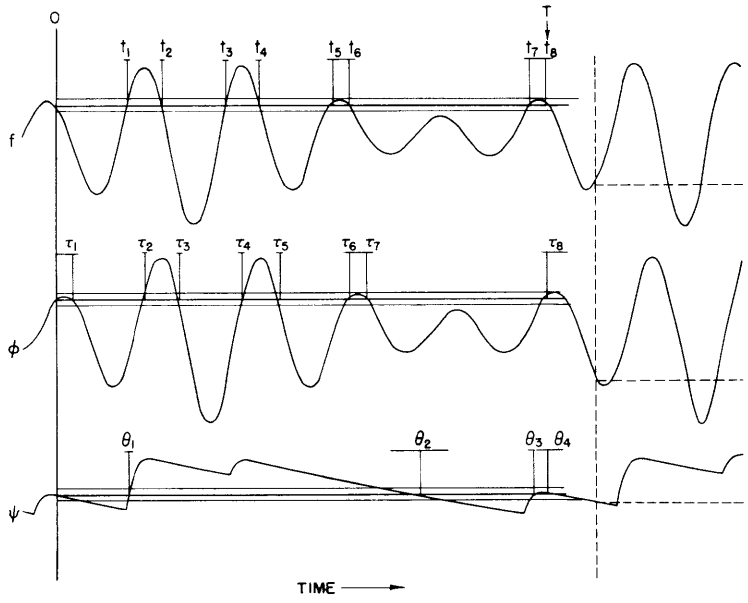

Fig. IX-5

Operation of the new pitchfinder on speech signals.

generally different from the times at which $f = f(0)$. Therefore, the period of the signal may be determined by observing the time at which $f = f(0)$ and $\phi = \phi(0)$ simultaneously.

In practice the signals are not exactly periodical, so that a tolerance must be allowed on the two equalities, $f = f(0)$ and $\phi = \phi(0)$. As a result, the probability of a false coincidence (not representing the period) increases. If this probability becomes too large, it can be decreased by detecting the coincidence for several functions rather than just two. In the example shown in Fig. IX-5, three functions are used. The function ϕ is obtained from f by a delay, the function ψ by a peak detection.

F. A. Muller

2. Statistical Theory of Natural Languages

A mathematical model presented by the writer to the London Symposium on Applications of Communication Theory in 1952 gave a possible information-theoretical representation and explanation of the experimental statistical data on words in natural languages. This model was based on certain empirical structural properties of languages and on the solution of the "inverse problem" of the theory of coding. For lack of experimental data, few further consequences of the model were stated.

During the past quarter the problem was reconsidered in a broader setting. Those properties of languages which were previously taken as experimentally established were all deduced theoretically from more elementary assumptions. In addition, new consequences of the model were drawn, which were later found to agree with experimental evidence.

A detailed account of this research, incorporating previous results, has been accepted for publication in Word.

B. Mandelbrot

C. HUMAN COMMUNICATION SYSTEMS

Dr. L. S. Christie
Dr. R. D. Luce
Dr. G. O. Rogge
J. Macy, Jr.
S. C. Bedard
L. M. deLeeuw
L. N. Lindgren
K. Ralston

1. Experiment on Network Change: Time Data

This experiment has been described in previous reports (1, 3). During the past quarter the IBM processing of the data was concluded and the analysis begun. In this report we shall discuss briefly one aspect of the individual time characteristics.

As it was pointed out in Technical Report No. 231 (4), if one assumes that a decision-making process is stimulated at time zero and that the probability a decision is made in the interval $(t, t + \Delta t)$, provided it has not been made earlier, is $\lambda(t)\Delta t$, then the distribution $f(t)$ of decisions is given by

$$f(t) = \lambda(t) \exp\left[-\int_0^t \lambda(x)dx\right]$$

In practice one observes

$$F(t) = \int_0^t f(x)dx$$

for discrete values of t, so $\lambda(t)$ must be estimated in terms of $F(t)$. If we let

$$\Lambda(t) = \int_0^t \lambda(x)dx$$

then

$$f(t) = \frac{d\Lambda}{dt} e^{-\Lambda}$$

Hence, integrating and solving for $\Lambda(t)$, we obtain

$$\Lambda(t) = -\log_e\left[1 - F(t)\right]$$

Differentiating, we find that

$$\lambda(t) = \frac{f(t)}{1 - F(t)}$$

which is not useful since it contains $f(t)$ which is not observed. We note that

$$\bar{\lambda} = \frac{1}{b-a} \int_a^b \lambda(t)dt = \frac{1}{b-a}\left[\lambda(b) - \lambda(a)\right] = \frac{1}{b-a} \log_e\left[\frac{1 - F(b)}{1 - F(a)}\right]$$

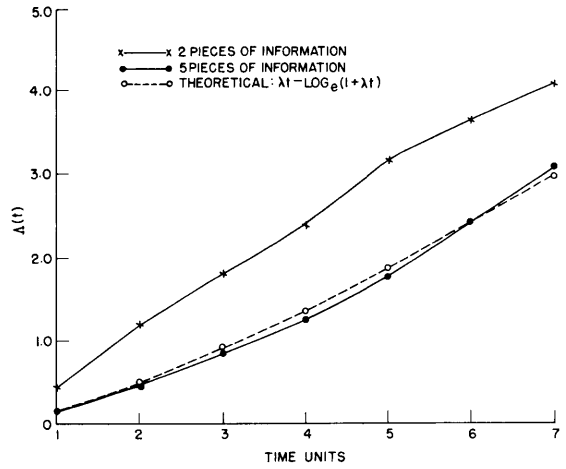

Fig. IX-6
Λ(t) for peripheral men, trial block 16-18.

is an estimate of λ(t), its average value in an interval, and contains only F(t). However, it is not suitable because it essentially preserves the derivative process as the ratio of two quantities, and so the estimate is very prone to error when applied to empirical data. To avoid this difficulty, we shall work with Λ(t).

The advantages of Λ(t) over the cumulative F(t) stem from the fact that in many decision-making processes the latency is approximately exponential, and so Λ(t) is approximately a straight line. Thus the comparison of two distributions, which may intersect one another, is transformed into the comparison of two nearly straight and nonintersecting lines, which is far easier.

For this experiment individual times were measured in two ways: the time interval between the message under consideration and the message sent immediately before it by the same person, and the interval from the given message to the most recent message received. Several arguments have been adduced to indicate the former process is basic, but they are too long to be reported here. In addition, one categorizes the data according to whether the individual is central or peripheral in the network diablo, and to the amount of problem information (one through five pieces) present at the time of sending. In Fig. IX-6 we present this data for the peripheral men during trial blocks 16 to 18 with two and five pieces of information present.

The principal features of the data are that Λ(t) is essentially a straight line when two pieces of information are present and that is is bowed when five are present. We shall suggest a relation between these two, which, though it is far from clearly formulated, suggests an interesting procedure for the study of decision processes.

Let us suppose there is such a thing as a psychologically "elementary decision" which is characterized by a latency f(t). Further, suppose any nonelementary decision is composed of some number n of elementary decisions which are executed serially. Then the latency $f_n(t)$ for the decision of complexity n is obviously given by

$$f_n(t) = \int_0^t \cdots \int_0^{\tau_2} f(\tau_1)\, f(\tau_2 - \tau_1) \cdots f(t - \tau_{n-1})\, d\tau_1 \cdots d\tau_{n-1}$$

If, in addition, we suppose $f(t) = \lambda e^{-\lambda t}$, then

$$f_n(t) = \frac{\lambda^n t^{n-1}}{(n-1)!} e^{-\lambda t}$$

and the corresponding $\Lambda(t)$ are λt and

$$\lambda t - \log_e \left[1 + \lambda t + \ldots (\lambda t)^{n-1}/(n-1)!\right]$$

For this experiment, the decision process involving two pieces of information present is sufficiently simple that one might suppose it is in some sense elementary. A more complicated decision problem exists when five pieces of information are present and we do not know the corresponding value of n. Observe, however, both the assumption that elementary decisions are additive and the assumption of a multiplicative breakdown, as given by information theory, yield n approximately 2. We shall suppose n = 2. Using the interval 1 to 5 (since the points for larger t are somewhat unreliable), we obtain $\lambda = 0.67$ for the case of two pieces of information present. Computing $\lambda t - \log_e (1 + \lambda t)$ for this case we obtain the dashed curve of Fig. IX-6. Considering there are no adjustable parameters in the equation, the fit is good, although the theoretical curve is more shallow than the observed.

We know very well that for these cases a good percentage of the time is devoted to the preparation of messages, and it is doubtful whether this should be treated as part of a decision process. It is certainly not implausible that a message containing twice as much information should require, on the average, twice as long to prepare. That we are also able to predict the change in shape of the distribution is more interesting. This problem appears to be of sufficient interest that more research should be carried out, but clearly this should not be done in the context of a group experiment in which numerous other factors are operating.

R. D. Luce

2. Experiment on Semantic Confusion

The design of this experiment has been previously reported (1). The experiment has been completed at Fort Devens, Massachusetts, using United States Army personnel. Seventy-two groups were run, 24 on each of three networks. The networks were Circle, Pinwheel, and Governor (4). The data from the experiment itself are in the process of analysis. Analysis of the Pre-Task Questionnaire has been completed and is reported below.

L. S. Christie, R. D. Luce, J. Macy, Jr., G. O. Rogge

3. Pre-Task Questionnaire

The construction of this questionnaire and the results of a factor analysis of it based on 100 subjects have been previously described (1). The questionnaire, with the addition of several new items, has been administered to 360 subjects who took part in the Semantic Confusion experiment. Factor analysis of these responses has confirmed the results of the first factor analysis. Furthermore, the delimitation of the factors measured by the questionnaire has been rendered considerably more precise.

L. S. Christie, G. O. Rogge

4. Action-Quantized Number Experiment: Time Data

In Technical Report No. 231 (4) we presented the time data from an experiment in which the last of five people determined the group time. With no other than intuitive justification, we assumed an exponential distribution and determined the constants t_o and λ by numerical minimization of χ^2. The resulting approximations were good.

Using the formulas outlined in section 1, we may check our assumption that $\Lambda(t)$ is a straight line. Let g(t) be the group time distribution, which is obtained from the individual distributions f(t) as the largest of n; that is

$$g(t) = n\, f(t)\, F^{(n-1)}(t) = \frac{d}{dt} F^n(t)$$

Thus

$$G(t) = F^n(t)$$

and so

$$\Lambda(t) - \log_e \left[1 - F(t)\right] = \log_e \left[1 - G(t)^{1/n}\right]$$

Using this expression and the indicated values of n (see reference 4 for their justification), we obtain for the circle network the results shown in Fig. IX-7. The straight lines are those obtained by minimizing the distribution χ^2.

R. D. Luce

5. Action-Quantized Number Experiment: Whirlwind Problem

In Technical Report No. 231 a model was outlined to describe the learning characteristics of this experiment, but because of mathematical difficulties it could not generally be solved. One special case was worked out, and the results were sufficiently in accord with the data that we were encouraged to attempt to solve it using Monte Carlo methods on Whirlwind. The coding problem has been described previously (2).

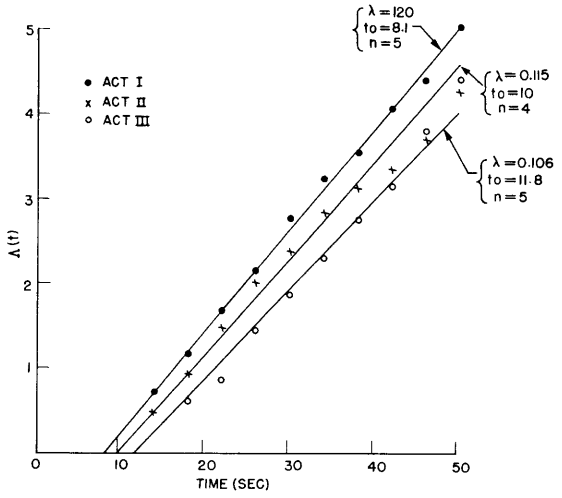

Fig. IX-7

Circle network, action-quantized experiment.

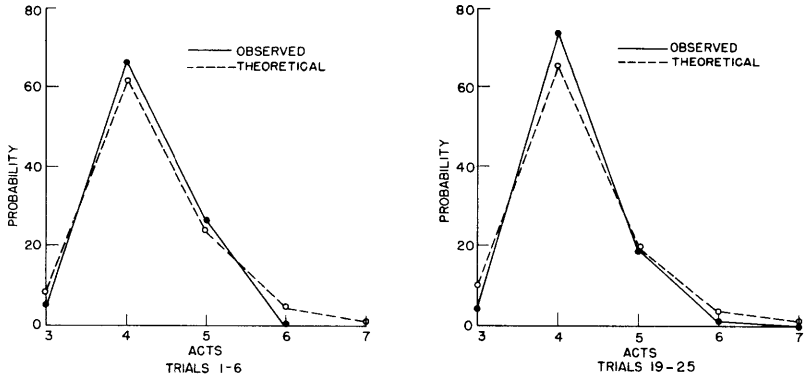

Fig. IX-8

Distributions of act to completion, pinwheel network.

One of the problems confronted was the generation of pseudo-random numbers. A scheme suggested by Wijngaarden was used. The recursion formula is

$$U_n = U_{n-1} + U_{n-k} \pmod{c}$$

where we used k = 7. Two checks were made on the distribution of these numbers and one to determine that cycling had not occurred in our range of interest, and they were deemed suitably "random."

One case of the model has been carried out during the quarter. This is shown in Fig. IX-8. It will be recalled that each trial of this experiment was completed in a discrete number of well-defined steps, called acts. Therefore, we have plotted the distribution of these acts for two trial blocks, the first and the last. The middle two trial blocks show results of the same quality. Several other cases will be run in the coming months.

R. D. Luce, K. Ralston

References

1. Quarterly Progress Report, Research Laboratory of Electronics, M.I.T. April 15, 1953, pp. 43-46
2. Quarterly Progress Report, Research Laboratory of Electronics, M.I.T. July 15, 1952, pp. 71-77
3. Quarterly Progress Report, Research Laboratory of Electronics, M.I.T. April 15, 1952, pp. 62-64
4. L. S. Christie, R. D. Luce, J. Macy, Jr.: Communication and Learning in Task-Oriented Groups, Technical Report No. 231, Research Laboratory of Electronics, M.I.T. 1953

D. VISUAL SENSORY REPLACEMENT PROJECTS

Dr. C. M. Witcher
L. Washington, Jr.

1. Further Work on Step-Down Detector

Work on this project during the past quarter has finally led to a seemingly satisfactory solution of the detection problem for wet weather conditions. The solution has not been field tested as yet, but experiments with very wet and with highly reflecting surfaces in the laboratory have yielded satisfactory step-down detection under all conditions.

The method for solving the problem was essentially that which was outlined in the Quarterly Progress Report of April 15, 1953: (a) the amplifier was completely redesigned to match the energy spectrum of the received signal; (b) the light source optics were somewhat improved by the use of a more accurately parabolic reflector; and (c) a more sensitive photo cell has been obtained.

As can be seen from the schematic, Fig. IX-9, the redesigned amplifier is fairly conventional, but the over-all consistency of the design produced enough improvement to permit the elimination of one stage. Note the replacement of the output transformer and half-wave diode rectifier by the arrangement which we have called a "diode pump" to furnish the dc voltage for biasing the grid of the alarm control tube. Note also that a shunt diode limiter has been incorporated in the plate circuit of the last stage. With this device a definite maximum value of the alarm bias voltage is established, no matter how great a signal amplitude the amplifier is receiving. The time constant of the alarm biasing circuit is now determined essentially by the 0.02 μf capacitor and the back resistance of one of the diodes, that is, 1.5 to 2.5 megohms. The action of the limiter insures that the response time of the alarm control circuit is held down to about the same order of magnitude as the bias circuit time constant.

The gain of the amplifier (the ratio of dc voltage across the diode pump capacitor to ac input voltage) is essentially flat from 20 to 100 cps and is about 70,000. It is down 6 db from this value at 150 cps and about 15 db at 200 cps. The limiter comes into operation at a dc output voltage of 10 to 12 volts, and most signals are strong enough to drive the output to this limiting value.

The use of a metal reflector on the light source instead of the former aluminized Bakelite type has, by its added moment of inertia, lowered the source vibration frequency to about 30 cps, and with this frequency it appears that the second and third harmonics are both well within the passband of the amplifier. The new reflector, provided through the courtesy of the Blake Manufacturing Company, Clinton, Massachusetts, gives considerable improvement in the light spot produced by the source on the basis of visual observation.

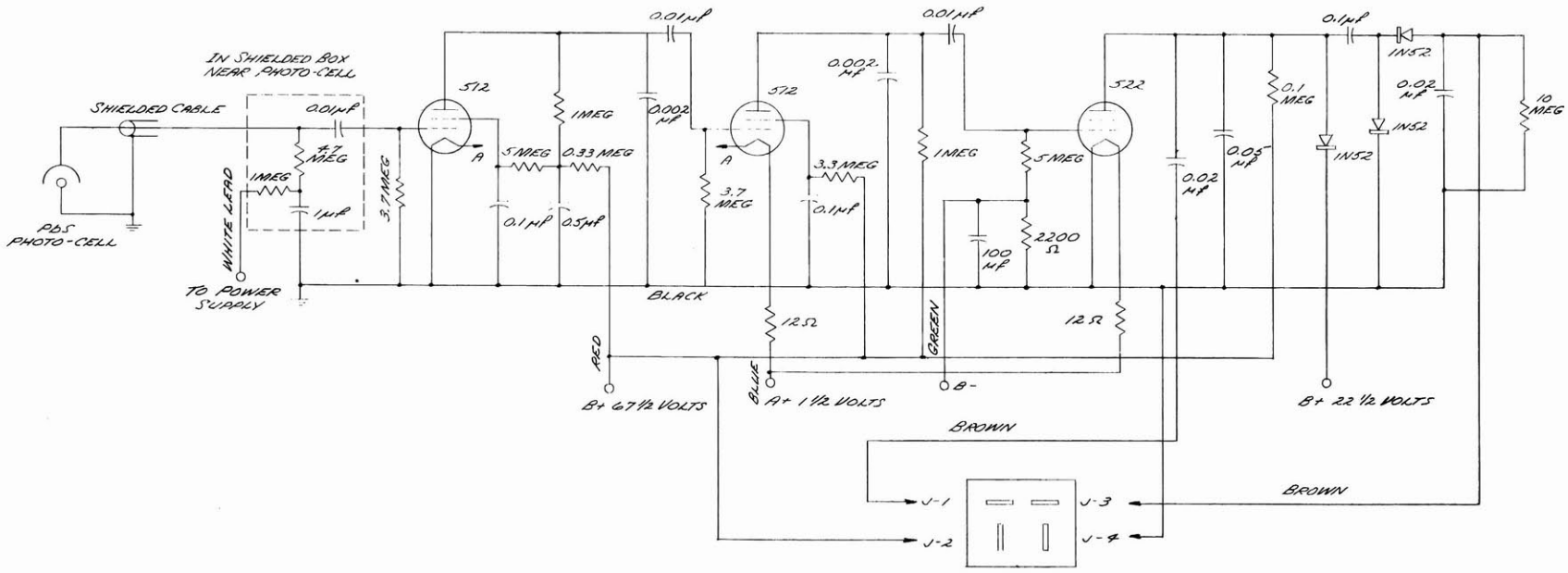

Fig. IX-9
Schematic of redesigned step-down detector.

During the course of this quarter's work the lead sulphide photo cell described previously has been replaced by a vacuum bulb cell in which the lead sulphide is evaporated on the inner surface of the glass. The active area of such a cell is delineated by two conducting electrodes, which are also located on the inner surface of the bulb. In the first cell these electrodes were 0.06 inch apart and 0.25 inch long. However, the cell was enclosed in a metal shield having a slit only 0.01 inch wide and 0.25 inch long. Thus the sensitivity of the cell was somewhat reduced, but even so, it gave satisfactory performance under very bad reflectivity conditions. As this is being written, two new cells have been received with interelectrode spacing of 0.01 inch and length of 0.25 inch, but they have not as yet been tested. It is felt that the end of the next quarter will see the step-down detection system in a state in which it operates reliably under all weather conditions. Incidentally, it appears that the use of the new very narrow photo cells, together with the limiter in the amplifier, will provide satisfactory signal dips at step-downs under all conditions of reflectivity without the need for any auxiliary system to control the gain of the amplifier as a function of terrain reflectivity.

2. Line and Pointer Locator

About two months ago we were requested by the American Foundation for the Blind, of New York City, to develop a simple means by which a blind person could detect the positions of pointers under glass or detect the boundaries of printed material on a page. The ability to locate pointers would allow the blind to engage in work involving the reading of meters and the like. The ability to detect ink lines or the boundaries of printed material would add to the types of work available to them. The solution which we obtained is extremely simple, and it is surprising indeed that it has not been attempted before. Actually, the principle is similar to that used some years ago by the Radio Corporation of America in a proposed reading device for the blind, but the circuit design and construction are vastly more simple.

A photograph of the final form of the device is shown in Fig. IX-10, and a circuit schematic is presented in Fig. IX-11. Basically, it consists of two small 0.04-watt neon lamps connected as relaxation oscillators. As the resistance element in one of the oscillators, a commercial lead sulphide photo cell is used, and a small potentiometer serves the same purpose for the other oscillator. Light from a small pen-light bulb located in one section of the v-shaped tube emerges from its apex through a small hole and is reflected back into the other side of the tube from whatever lies outside the hole. The reflected light, after passing through a lens, is focused on the photo cell. Variations in the reflected light will produce small variations in the cell resistance, and hence small variations in the frequency of the oscillator of which it is a part. The second oscillator can be tuned to zero beat with the cell oscillator for any given light intensity,

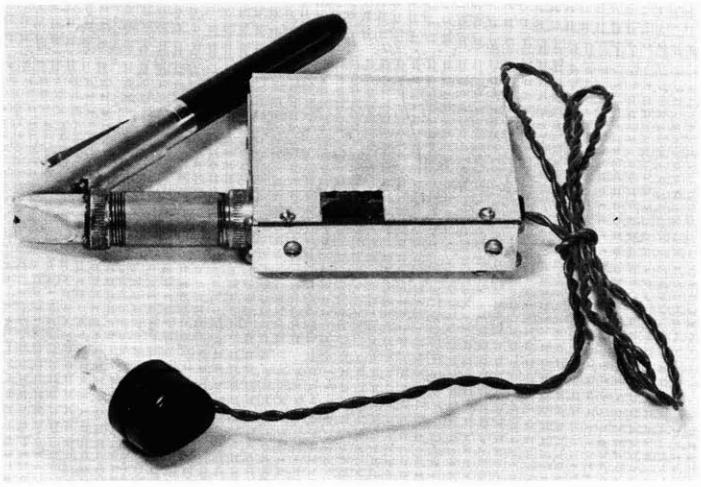

Fig. IX-10
Line and pointer locator.

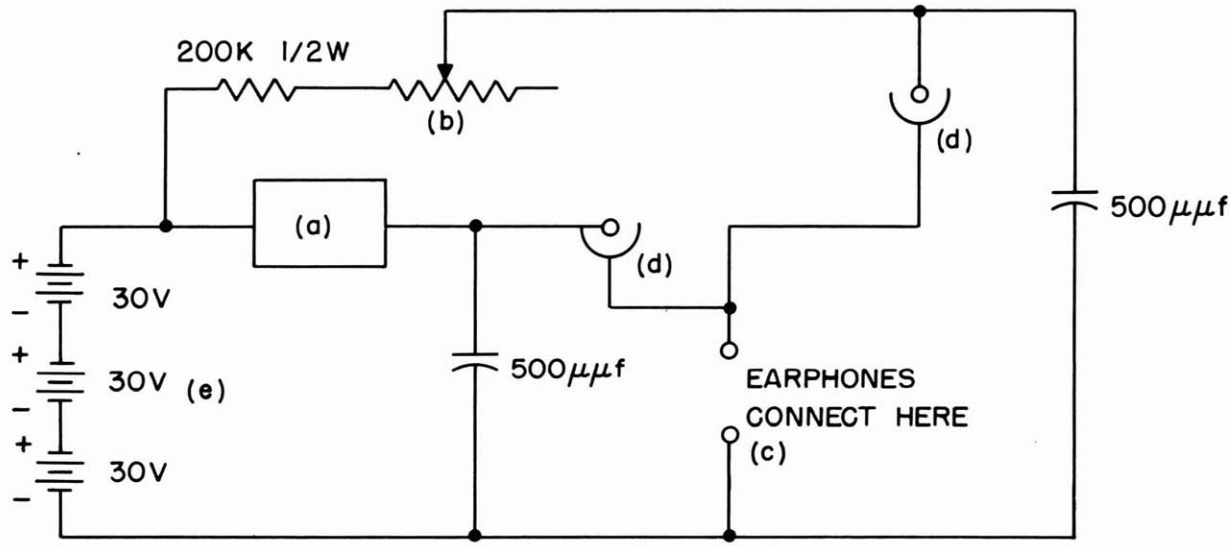

Fig. IX-11

Schematic of line and pointer locator. (a) Lead sulphide photo cell (Photoswitch, Inc., No. A 4-116), button-type, sensitivity > 50 db, 1 to 2 megohms. (b) Centralab 3-megohm potentiometer B116-224. (c) Earphones "R-30-U" or equivalent (50 to 70 ohms dc). (d) Neon tubes Ne-2, 1/25 watt. (e) 30-volt "B" battery, Eveready 507E.

and a very slight change in light intensity will then produce a distinct beat frequency. The small amount of coupling provided by the common impedance of the batteries and earphone tends to decrease the sensitivity of the system slightly, but it also makes it easier to set to zero beat. The present unit is sensitive enough to detect most printing without difficulty and to detect the positions of meter pointers easily. When used to locate pointers, the v-tube shown is replaced by one in which the apex has been milled off so that the point of maximum sensitivity of the system is approximately 0.312 inch out beyond the opening at the common end of the tubes. The expected life of the type 507E Eveready batteries in this device is 500 to 700 hours, the total drain being only about 30 μa.

E. SPEECH ANALYSIS*

Prof. M. Halle
G. W. Hughes
Carol D. Schatz
C. P. Smith

1. Analysis of Voiced Sounds

Since the last Quarterly Progress Report, attention has been focused on the voiced stop and fricative sounds. A voiced sound may consist of two components, $f_1(t)$ and $f_2(t)$: $f_2(t)$ is produced by the upper vocal tract constrictions at the lips, teeth, and the like, and $f_1(t)$ is a periodic voicing component produced by the vocal chords. The information as to onset time is carried by $f_2(t)$, which is generally masked by the very strong voicing component $f_1(t)$. In order to apply stop-distinguishing vs fricative-distinguishing criteria such as those described in the last report, $f_2(t)$ must be separated from $f_1(t)$. Experimental evidence indicates that the combination of $f_1(t)$ and $f_2(t)$ is not additive but one of modulation or multiplication. Thus the acoustical speech wave for the voiced sounds would be not of the form $K_1 f_1(t) + K_2 f_2(t)$ but rather $K_3 f_1(t) + K_4 f_1(t) f_2(t)$, where the K's are numerical constants, and the first term in the last expression accounts for the large amount of voicing that appears unaffected by constrictions.

Since the frequency components of $f_2(t)$ are generally higher than those of $f_1(t)$, a division of the output of a highpass filter by that of a lowpass filter should produce an approximation to $f_2(t)$. Various schemes for performing the division continuously have been considered.

An easily constructed speech sampler-quantizer has been built so that the digital computer, Whirlwind I, can operate on the speech wave. The unit samples simultaneously the rectified outputs of the highpass and lowpass filters 10,000 times per second, quantizes the waveforms to one part in 140, and feeds this digital information into Whirlwind's storage. The computer can then be programed to perform any analytical operation on this information and display the result visually. So far, results on the division process to separate $f_2(t)$ are inconclusive but promising.

G. W. Hughes, M. Halle

2. Perception of Artificially Combined Speech Sounds

a. Effect of the following vowel on the perception of stop consonants

In order to determine the effect of context change on the perception of prevocalic stop consonants, tape-recorded stops have been cut away from the vowels before which they were pronounced and spliced back before other vowels. The effect on perception

*The work reported in this section was also supported in part by the Carnegie Foundation and the Rockefeller Foundation.

of such recombinations for the consonant [k] was reported in the Quarterly Progress Report, January 15, 1953. Tests have now been completed for [p] and [t], and a variation of the experiment for [k] has been carried out.

Tape recordings were made of an American speaker pronouncing the syllables [pi], [pa], [pu], and the vowels [i], [a], and [u]. The [p]'s were then cut away from the vowels before which they were pronounced at the point where the voicing of the vowel begins, approximately 50 msec after the beginning of the syllable. Each [p] was cut away from its own vowel and spliced back before [i], [a], and [u]. For [k], recombinations using the entire consonant yielded unnatural sounding syllables, and produced no changes in perception; it was only when the 10 to 15 msec consonantal burst alone was used that the syllables sounded acceptable and perceptual changes occurred. For [p], however, combinations using the entire consonant produced acceptable syllables, and using only the burst decreased, rather than increased, the tendency toward perceptual changes. The results presented here are therefore based on combinations made with the entire consonant.

Five samples were made up of each of the nine combinations (the [p]'s from [pi], [pa], and [pu], each combined with the three vowels), and these syllables were presented in random order to 20 subjects who were asked to identify the initial consonant as [p], [t], or [k]. Figure IX-12 shows the subjects' identifications of the consonants in each one of these combinations. In each case the percentage of [p] responses was greater than that of either [k] or [t], and the conclusion can be drawn that changes in perception due to changes in the following vowel do not occur for [p] as they do for [k]. It should

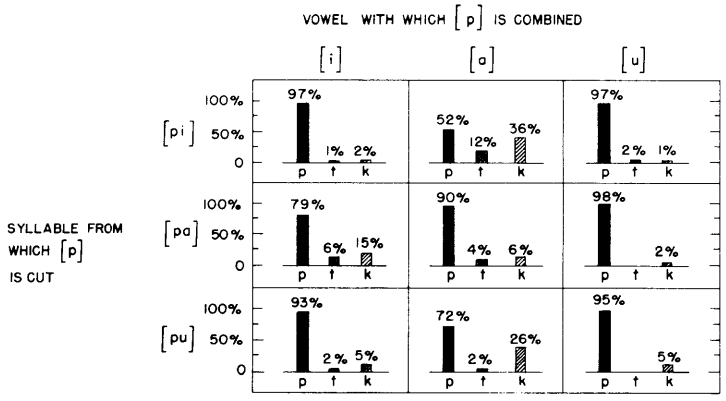

Fig. IX-12

Consonant identifications in syllables made up of initial [p]'s combined with [i], [a], and [u]. The figures indicate percentage response for 20 subjects to five samples of each combination.

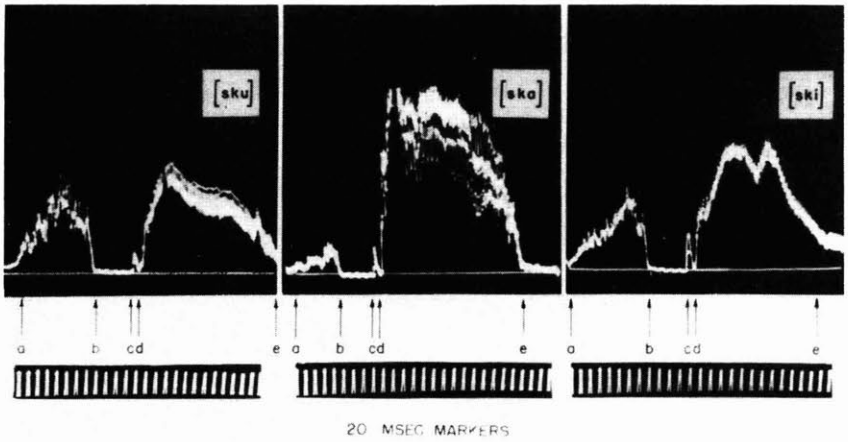

Fig. IX-13

Oscillograms of the syllables [sku], [ska], and [ski]. The [s] (a-b) is followed by silence (b-c). The [k] explosion (c-d) is followed directly by the vowel (d-e).

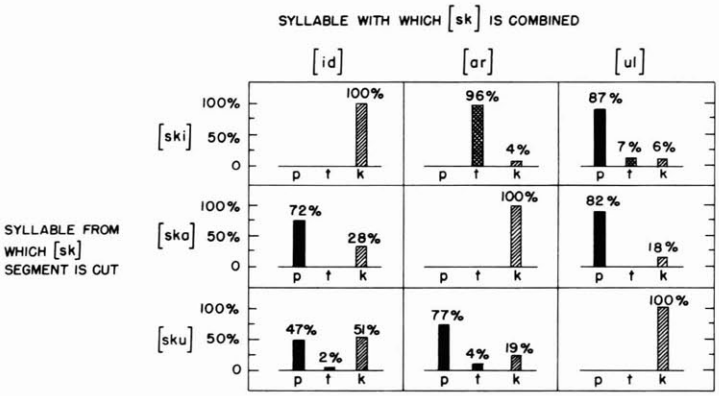

Fig. IX-14

Stop consonant identifications in syllables made up of initial [sk] segments combined with [i], [a], and [u]. The figures indicate percentage response for 20 subjects to five samples of each combination.

be noted, however, that in the combinations [pi] and [a], [pu] and [a] (and to a lesser extent, [pa] and [i]), the percentage of p responses is lower than in the other cases (as low as 52 percent for [pi] and [a]), and the percentage of [k] responses greater (36 percent for [pi] and [a]). This is of interest in that according to our data for [k], we would predict changes in perception in these combinations. Since the percentage of [k] responses is higher in these combinations than in the remaining ones, there is some tendency for [p] to be heard as [k] in these positions.

The same experiment was run for the consonant [t], using [t]'s from the syllables [ti], [ta], and [tu], and splicing them back before [i], [a], and [u]. As for [p], transposing the entire consonant produced natural sounding syllables. Testing showed that the [t]'s were perceived as [t]'s in all combinations, and the percentage response varied very little for combinations made using the entire consonant and combinations using only the initial burst.

A variation of the experiment was carried out for [k]. Instead of using aspirated [k]'s and cutting away the aspiration to retain only the initial burst, [k]'s were used from the syllables [ski], [ska], and [sku] (see C. D. Schatz: Quarterly Progress Report, Research Laboratory of Electronics, M.I.T. Jan. 15, 1953, pp. 38-39). Here the [k] is not aspirated and the vowel begins directly after the burst. Figure IX-13 shows oscillograms of [ski], [ska], and [sku], in which (d) indicates the point at which the burst ends and the vowel begins. The [sk] segment was cut away from the syllables [ski], [ska], and [sku] at (d) in Fig. IX-12, and spliced back before [i], [a], and [u]. Subjects were instructed to identify the initial portion of the syllables as [sp], [st], or [sk]. Figure IX-14 shows the subjects' identifications of the consonants in each one of these combinations. The results agree with those previously reported for the burst of aspirated [k]. The consonants were identified as [k] when transposed before a vowel similar to the one they originally preceded. Thus perceptual changes for other combinations can be attributed to context, and not to factors introduced by the mechanics of cutting and recombining. Transposed, the [k]'s were perceived in four combinations as [p], in one combination as [t], and in one combination as approximately 50 percent [p] and 50 percent [k].

Carol D. Schatz

F. TRANSIENT PROBLEMS

Prof. E. A. Guillemin
Dr. M. V. Cerrillo
Dr. F. M. Reza
F. Ba Hli
E. F. Bolinder
R. A. Pucel

1. Methods of Integration: Notes on the "Cliff" Method*

1.0 Introduction. This report presents a compact general description of the "cliff" method of approximate integration. Due to space limitation the main ideas on which the method is based and the procedure to be followed will be presented in concise form. The method will be explained here in terms of its application to a specific set of integrals. The integrals chosen represent the radiation field from a dipole, vertical or horizontal, in the presence of a plane earth with finite conductivity. Among these integrals we select the ones representing the different Hertz potentials. One of them will be directly evaluated in this report. The other integrals of the set can be treated along similar lines.

We will produce approximate integral solutions for one of the Hertz potentials. The solutions will be valid in the near-field region, not necessarily small, around the dipole. The solutions are obtained as rapidly and uniformly convergent series.

The cliff method can also be used to obtain approximate solutions which are valid at medium or at far distances from the dipole. The briefness of this report will, however, not allow us to discuss these possibilities. In connection with the integrals selected here the required procedure is rather simple.

1.1 The cliff method of approximate integration attempts to find directly approximate solutions of integrals which must be integrated along and around the branch cuts of the integrand functions. The name "cliff" is adopted because of the discontinuous aspect of a three-dimensional plot of some elements of the functions over the plane of the variable. By standing on one sheet of the Riemann manifold, the isometric plot of the real or of the imaginary part of the function, one of which (or both) is always discontinuous, will resemble the typical aspect of a cliff along the branch cut. A visual illustration of such a cliff can be found, for example, in reference 1 (pp. 52, 55, 91, etc.). Some cliffs associated with elliptic functions are shown in Exhibit 1, which is copied from reference 1.

1.2 The fundamental idea on which the cliff method of approximate integration is founded can be described in a concise manner, as follows:

Let the integrand be a multivalued function. For simplicity in the explanation let us assume

a. that the contour of integration runs completely in one, and only one, sheet of the

---

*Summary of a paper given at the Symposium on Microwave Optics, McGill University, Montreal, June 22-25, 1953.

Riemann manifold, and

b. that the contour of integration may be deformed into an equivalent one around certain pertinent singularities and branch cuts of the integrand.

For convenience we will illustrate this situation by a simple example. Take the integral

$$f(t) = \frac{1}{2\pi i} \int_{\gamma} \frac{e^{st}\, ds}{(1 + s^2)^{1/2}} \quad ; \quad F(s) = \frac{1}{(1 + s^2)^{1/2}}$$

where the contour γ of integration runs in one Riemann sheet, say Sheet I, of the manifold corresponding to $(1 + s^2)^{1/2}$. See Fig. IX-15(a). The contour γ can be deformed around the branch cut, having branch points at $s = \pm i$. The above integral can be evaluated by the direct integration around the branch cut.

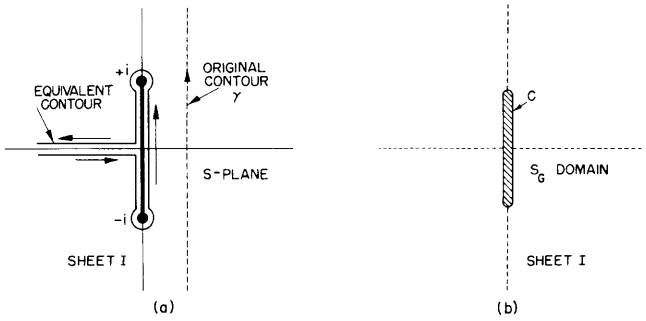

Fig. IX-15

(a) Contour of integration around the cut. (b) Definition of S_G.

Now we proceed with some preparatory steps towards the construction of the cliff method of integration.

a. Let us define the open domain S_G as follows. Take the S-plane and exclude the shaded regions and their boundaries around the branch cut. See Fig. IX-15(b). The domain S_G is a multiple-connected region.

b. A function M(s) is introduced as follows:

1. M(s) is defined only in S_G.
2. M(s) has natural boundaries at the contour C.
3. M(s) is a single-valued function of $s \in S_G$ such that M(s) ≡ Branch I of F(s) for $s \in S_G$. M(s) may not exist for $s \notin S_G$ and does not represent F(s) in the shaded regions.

The proof of existence and construction of the function M(s) is outside the scope of this report. We will limit ourselves to indicating a method of construction of the

function M(s) which represents the function F(s) in the example above.

1.3 There are an infinite number of ways to produce such a function M(s). For simplicity we will indicate a method based on continued-fraction expansions. At the same time the concept of "intrinsic" cut will be introduced.

Let us consider the multivalued factor $(1 + s^2)^{1/2}$ and select the branch associated with the positive value of the radical.

It can be shown that this branch can be expressed by the continued-fraction expansion

$$+(1 + s^2)^{-1/2} = \cfrac{1}{1 + \cfrac{1}{2s^2 + \cfrac{1}{2 + \cfrac{1}{2s^2 + \cfrac{1}{2 + \ddots}}}}}$$

The first few approximants are given by

$$\frac{A_1}{B_1} = 1 \quad ; \quad \frac{A_2}{B_2} = \frac{2s^2}{2s^2 + 1} \quad ; \quad \frac{A_3}{B_3} = \frac{4s^2 + 1}{4s^2 + 3} \quad ; \quad \frac{A_4}{B_4} = \frac{8s^4 + 4s^2}{8s^4 + 8s^2 + 1}$$

The following general properties are of interest here:

a. The continued-fraction expansion converges uniformly towards $+(1 + s^2)^{-1/2}$ for every value of s, except for the segment of the imaginary axis between +i and -i.

b. The zeros and poles of every approximant lie in the interval (+i, -i).

c. The zeros and poles of every approximant interlace, forming a pole-zero chain.

d. Let n be the order of an approximant. The number of poles and zeros becomes dense everywhere in the interval (+i, -i), when $n \to \infty$, in such a way that

1. no point is a point of accumulation of zeros or of poles, and

2. the distribution function associated with such a pole-zero chain remains finite and well determined, when $n \to \infty$.

The reader may observe: (a) the single-valued character of every approximant and (b) that the segment (+i, -i) becomes a natural boundary of the function defined by the continued-fraction expansion because of the dense character of the poles. No analytical continuation is possible.

The approximants define a sequence of rational functions which approximate the branch of the radical. The particular representation is valid if, and only if, the branch cut is drawn as in Fig. IX-15. If the branch cut is changed, then the rational representation must be changed accordingly. The line on which the pole-zero chain lies is called the "intrinsic cut" of the rational representation.

1.4 An elementary description of the cliff method of integration can now be given. The previous integral will be used.

Suppose that we approximate the function $+(1 + s^2)^{-1/2}$ by the n-th approximant A_n/B_n of the continued fraction. The integration around the cut is now reduced to the integration around the poles of A_n/B_n. The Cauchy residue theorem produces immediately the solution of the integral. See Fig. IX-16. By this simple procedure it can be shown that

$$f(t) \approx 0.333 \cos 0.5t + 0.18332 \cos 0.17364t$$
$$+ 0.43093 \cos 0.9397t + 0.05197 \cos 0.766t$$

This solution provides a very good approximation in the interval $0 \leqslant t < 6$.

For very large values of t the cliff method yields the expression

$$f(t) \approx \frac{\cos\left[t - (\pi/4)\right]}{\left[(\pi t)/2\right]^{1/2}}$$

(Note that the exact solution of the integral is $f(t) = J_o(t)$.)

2.0 The following sections deal with the presentation of the results of a typical integral associated with the problem of radiation of a dipole in the presence of a finitely conductive plane earth.

We consider the integral

$$I_x = \int_{\gamma(\lambda)} H_o^{(1)}(\lambda r) \cdot e^{-\mu(z+h)} \frac{\lambda d\lambda}{\mu + \mu_E}$$

which represents the x component of the Hertz potential of the field from a horizontal dipole above the ground. In order to save space, we refer the reader to reference 2, where the set of integrals representing the different potentials is given. (See especially Eqs. 12(a), (b), (c) and 15, section 23, page 259.) The same symbols will be used as in the reference. For briefness, details of notation will be omitted in this report.

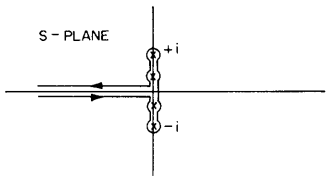

Fig. IX-16
Integration around the poles.

By $\gamma(\lambda)$ we will understand the contour of integration in the λ-plane, along which the function I_x is defined. The fundamental $\gamma(\lambda)$ contour runs along the real axis of the λ-plane, from $-\infty$ to $+\infty$, dodging the branch points in the manner indicated in reference 2, Fig. 28, page 251, Generally speaking, $\gamma(\lambda)$ will denote any other contour which is topologically equivalent to the one mentioned above. The contour of integration which is suitable for the application of the cliff method will be given in a later section.

2.1 We will use normalized units. They are defined as

$$w = \frac{\lambda}{k} \; ; \qquad \sigma = k(z+h) \; ; \qquad \text{and} \qquad kr = \rho$$

Then

$$I_x = k \int_{\gamma(w)} H_o^{(1)}(\rho w) \cdot e^{-\sigma(w^2-1)^{1/2}} \frac{wdw}{(w^2 - 1)^{1/2} + (w^2 - n^2)^{1/2}} \tag{1}$$

where $\gamma(w)$ indicates the transformed contour of integration in the w-plane. Final results will be given in terms of these normalized units.

A second transformation is used in order to bring out some important analytical characteristics of the functions forming the integrand. This transformation is given by

$$(w^2 - 1)^{1/2} = -iu \; ; \qquad i = (-1)^{1/2} \tag{2}$$

Then

$$I_x = -ik \int_{\gamma(u)} \left\{ H_o^{(1)}\left[\rho(1 - u^2)^{1/2}\right] \right\} e^{i\sigma u} \left[F(X)\right] du \tag{3}$$

where

$$F(X) = \frac{1}{1 + \left(1 + \frac{1}{X}\right)^{1/2}} \; ; \qquad X = \frac{u^2}{n^2 - 1} \tag{4}$$

$\gamma(u)$ is the transformed contour of integration. The cliff method will now be applied directly to the integral of Eq. 3. The contour is deformed around the "intrinsic cuts." Figure IX-17 shows the branch cuts and the deformation of the contour of integration in the different planes.

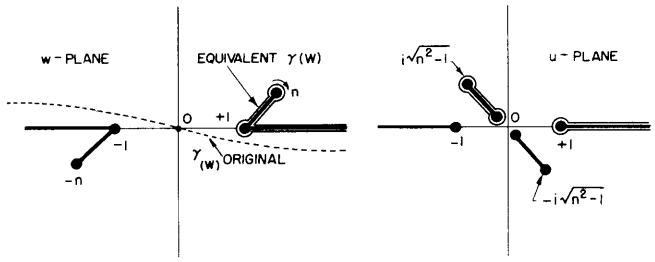

Fig. IX-17
Equivalent contour of integration around the cuts in the w- and u-planes.

2.2 The integrand in Eq. 3 has been strategically separated into the multivalued factors $H_o^{(1)}\left[\rho(1 - u^2)^{1/2}\right]$ and F(X). The first factor leads to a zero-pole chain contained in the intrinsic cut $\left[+i(n^2 - 1)^{1/2}, 0\right]$. See Fig. IX-17. The argument of $H_o^{(1)}$ produces a pole-zero chain from +1 to $+\infty$ and from -1 to $-\infty$. We need only the chain from +1 to $+\infty$. The function $H_o^{(1)}\left[\rho(1 - u^2)^{1/2}\right]$ produces a chain of essential singularities of exponential and logarithmic type.

2.3 Monogenic representation of F(X). The condensed results are

a. Continued fraction.

$$F(X) = \cfrac{1}{2 + \cfrac{1}{2X + \cfrac{1}{2 + \cfrac{1}{2X + \ddots}}}} \tag{5}$$

(intrinsic cut $-1 < X < 0$, X real).

b. Sequence of approximants.

$$F_p(X) = \frac{A_p}{B_p}, \qquad p = \text{order of approximant}$$

The first few approximants are

$$F_0(X) = \frac{1}{2} \qquad F_3(X) = \frac{2X^2 + X}{4X^2 + 3X + \frac{1}{4}}$$

$$F_1(X) = \frac{2X}{4X + 1} \qquad F_4(X) = \frac{1}{2}\,\frac{X^2 + \frac{3}{4}X + \frac{1}{16}}{X^2 + X + \frac{3}{16}} \tag{6}$$

$$F_2(X) = \frac{4X + 1}{2(4X + 2)} \qquad F_5(X) = \frac{1}{2}\,\frac{X^3 + X^2 + \frac{3}{16}X}{X^3 + \frac{5}{4}X^2 + \frac{3}{8}X + \frac{1}{64}}$$

c. Poles and zeros. Let

n_p = number of zeros of A_p

m_p = number of poles of $F_p(X)$ (zeros of B_p)

$\mathring{X}_{j,p}$ = j-th zero of A_p $(j = 1, 2, \ldots, n_p)$

$\overset{x}{X}_{k,p}$ = k-th pole of $F_p(X)$ $(k = 1, 2, \ldots, m_p)$

For example, the zeros and poles of the fifth approximant are

$$\overset{\circ}{X}_{1,5} = 0 \qquad \overset{\circ}{X}_{2,5} = -\frac{1}{4} \qquad \overset{\circ}{X}_{3,5} = -\frac{3}{4}$$

$$\overset{x}{X}_{1,5} = -0.0495156 \qquad \overset{x}{X}_{2,5} = -0.3887395 \qquad \overset{x}{X}_{3,5} = -0.811745 \tag{7}$$

d. Partial-fraction expansion of the approximants. The partial-fraction expansion of the approximants will be denoted by

$$F_p(X) = \frac{A_p}{B_p} = \frac{1}{2} - \sum_{k=1}^{m_p} \frac{L_{k,p}}{X - \overset{x}{X}_{k,p}} \tag{8}$$

where $L_{k,p}$ is the residue of the pole at $\overset{x}{X}_{k,p}$. For example, we get for the fifth approximant

$$F_5(X) = \frac{1}{2} - \frac{0.01348}{X - \overset{x}{X}_{1,5}} - \frac{0.0683}{X - \overset{x}{X}_{2,5}} - \frac{0.04418}{X - \overset{x}{X}_{3,5}} \tag{9}$$

2.4 By the direct application of the residue theorem we obtain for the contribution of the integral around the branch cut between +n and +1 the following uniformly convergent series:

$$I^*_{1,p} = i\pi k(n^2 - 1)^{1/2} \sum_{k=1}^{m_p} \frac{L_{k,p}}{\left[\left|\overset{x}{X}_{k,p}\right|\right]^{1/2}} \times H_o^{(1)}\left\{\rho\left[1 + (n^2 - 1)\left|\overset{x}{X}_{k,p}\right|\right]^{1/2}\right\} \exp\left\{-\sigma\left[(n^2 - 1)\left|\overset{x}{X}_{k,p}\right|\right]^{1/2}\right\} \tag{10}$$

where $I^*_{1,p}$ denotes the contribution corresponding to the p-th approximant along the cut (+n, +1) in the w-plane.

2.5 We will now prepare the notation required for the evaluation of the integral along the cut from +1 to +∞ in the w-plane. We start with the monogenic representation of the argument $(1 - u^2)^{1/2}$ along the cut from +1 to +∞.

a. Continued-fraction expansion. We write

$$(1 - u^2)^{1/2} = (1+u)^{1/2} \cdot (1-u)^{1/2}$$

and

$$(1-u)^{1/2} = 1 - \cfrac{\frac{u}{2}}{1 - \cfrac{\frac{u}{4}}{1 - \cfrac{\frac{u}{4}}{1 - \ddots}}} \tag{11}$$

(intrinsic cut $+1 \leqslant u < \infty$, u real).

b. Sequence of approximants.

Let S_q/R_q denote the q-th approximant of Eq. 11.

For example, the fifth approximant is given by

$$\frac{S_5}{R_5} = \frac{-u^3 + 18u^2 - 48u + 32}{6u^2 - 32u + 32} \tag{12}$$

c. Poles and zeros. We will use the analogous notation $\mathring{u}_{j,q}$ and $\overset{x}{u}_{k,q}$ to denote the zeros and poles of the approximants, respectively. For example, the poles and zeros for q = 4 are

$$\left.\begin{aligned} \mathring{u}_{1,4} &= 2\left[1 + \frac{1}{(5)^{1/2}}\right] & \mathring{u}_{2,4} &= 2\left[1 - \frac{1}{(5)^{1/2}}\right] \\ \overset{x}{u}_{1,4} &= 2\left[3 + (5)^{1/2}\right] & \overset{x}{u}_{2,4} &= 2\left[3 - (5)^{1/2}\right] \end{aligned}\right\} \tag{13}$$

d. Partial-fraction expansion. The partial-fraction expansion of the q-th approximant S_q/R_q can be written as

$$\left.\begin{aligned} \frac{S_q}{R_q} &= \epsilon_q u + k_q + \sum_{k=1}^{t_q} \frac{N_{k,q}}{u - \overset{x}{u}_{k,q}} \\ \text{where} \quad \epsilon_q &\begin{cases} = 0 & \text{for q even} \\ \neq 0 & \text{for q odd} \end{cases} \end{aligned}\right\} \tag{14}$$

For example, the partial-fraction expansion of the fourth approximant reads

$$\frac{S_4}{R_4} = 5 + \frac{\frac{44}{(5)^{1/2}} + 20}{u - \overset{x}{u}_{1,4}} + \frac{\frac{44}{(5)^{1/2}} - 20}{u - \overset{x}{u}_{2,4}} \tag{15}$$

2.6 For the integration along the cut (+1, +∞) in the u-plane, the residue theorem cannot be used because the function $H_o^{(1)}$ has an essential singularity at a zero of S_q and an algebraic pole of order 1/2 at the zeros of R_q. The integration around these singularities can, however, be performed by direct methods. Since they are rather involved, we will omit them in this report, so that only final results will be given.

It can be shown that the contribution to the integral along the second cut, from +1 to +∞, is given by the uniformly convergent series

$$I^*_{2,q} = \frac{8}{3}\, 2^{1/2}\, \rho i k \sum_{k=1}^{t_q} N_{k,q}\, \frac{\overset{x}{u}_{k,q}(1+\overset{x}{u}_{k,q})^{1/2}\exp(+i\sigma\overset{x}{u}_{k,q})}{\overset{x}{u}_{k,q}+\left[\overset{x}{u}{}^2_{k,q}+(n^2-1)\right]^{1/2}}$$

$$\times \Lambda_{3/2}\left\{2\left[\rho N_{k,q}\,\sigma(1+\overset{x}{u}_{k,q})^{1/2}\right]^{1/2}\right\} \tag{16}$$

where t_q is the number of poles of the q-th approximant of Eq. 11. $\Lambda_{3/2}$ is the Lambda function of order 3/2. See section 2.8.

2.7 The solution of the integral of Eq. 1 is therefore given by

$$I_x \approx I^*_{1,p} + I^*_{2,q} \tag{17}$$

The solutions (Eqs. 10 and 16) converge very fast for large values of σ and ρ. A complete discussion of these results will be given in a section of Technical Report No. 55.

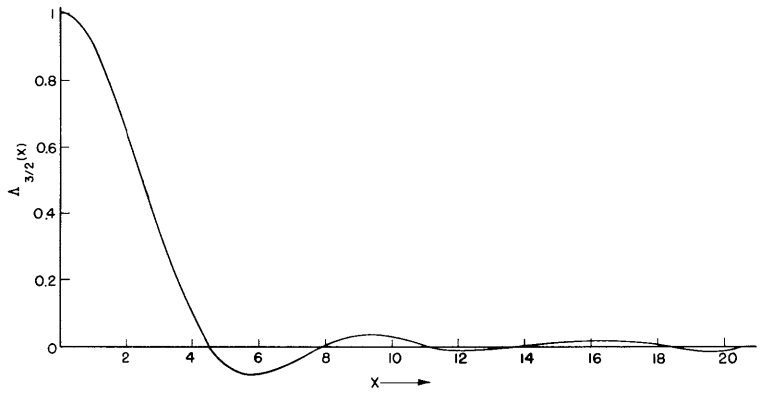

Fig. IX-18
Graph of the Lambda function of order 3/2.

2.8 We close this report with the definition of the Lambda function, which is given in Eq. 16. The Lambda function $\Lambda_\nu(z)$ of order ν is defined by

$$\Lambda_\nu(z) = \Gamma(\nu+1)\,\frac{J_\nu(z)}{\left(\frac{z}{2}\right)^\nu}$$

In Eq. 16 the argument is real. Let

$$x = 2\left[\rho N_{k,q}\,\sigma(1+\overset{x}{u}_{k,q})^{1/2}\right]^{1/2}$$

The graph of the function $\Lambda_{3/2}(x)$ is given in Fig. IX-18.

EXHIBIT 1

Examples of Functions Showing Cliffs

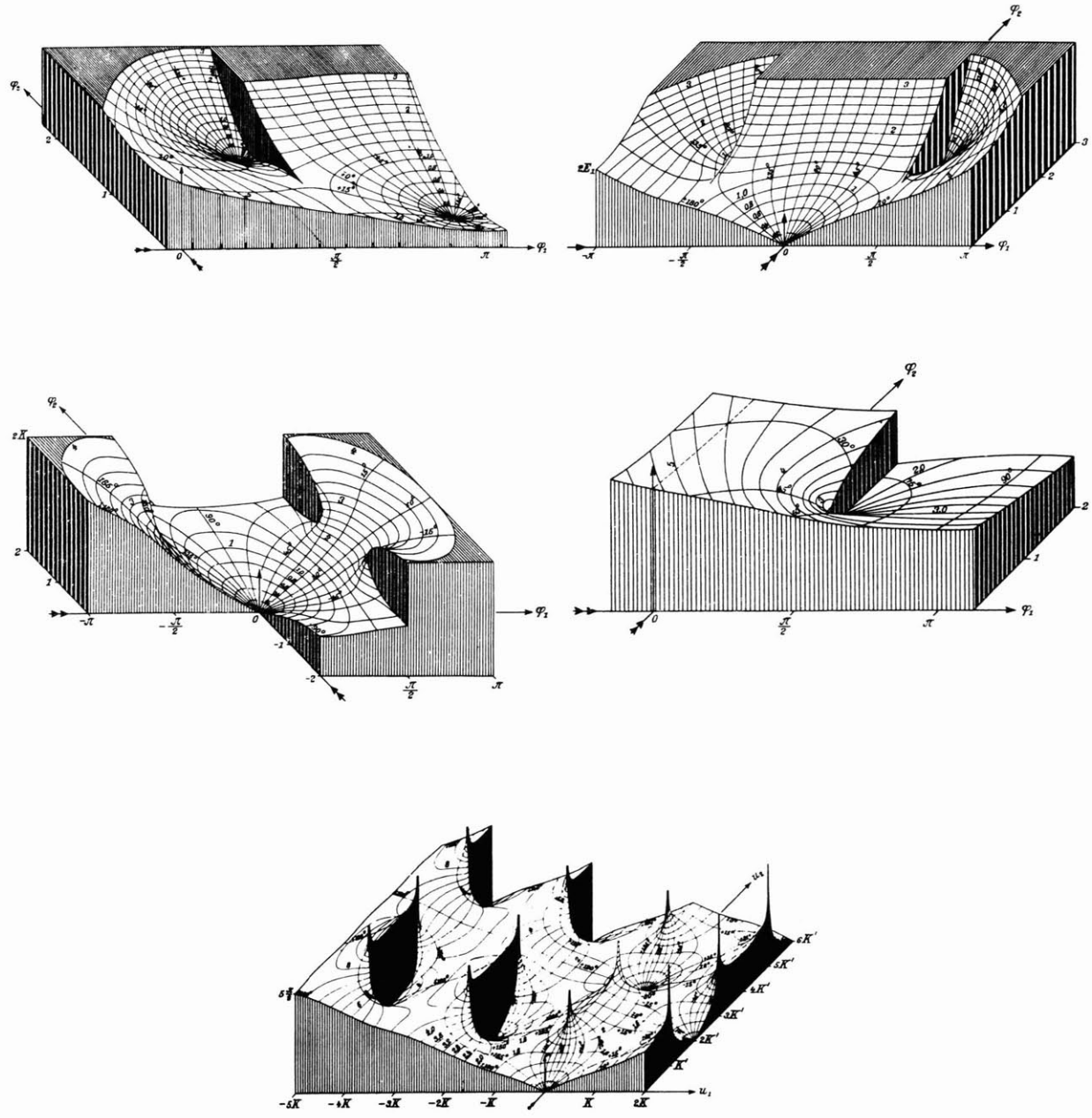

APPENDIX

In the presentation above of the cliff method we have used continued-fraction expansions of the functions $(1-u)^{1/2}$ and F(X). This was done because we want to keep the presentation in familiar mathematical terms. The cliff method does not require the use of continued fractions. The fundamental expansion procedure basically rests on the introduction of distribution functions along the cuts. In the verbal presentation of this material at the Montreal Symposium on Microwave Optics, distribution functions were used. Exhibit 2 shows a condensation of the method of distribution functions. (The procedure was presented on two of the slides at the Symposium.) For lack of space we cannot go into more detail; however, a detailed explanation will appear in a section of Research Laboratory of Electronics Technical Report No. 55.

EXHIBIT 2

General Procedure to Construct the Monogenic Function by using Distribution Functions Instead of Continued-Fraction Expansions

I. Consider, for example, the integral

$$\prod_x = k \int_{\gamma(w)} H_o^{(1)}(\rho w) \exp\left[-\sigma(w^2 - 1)^{1/2}\right] \frac{w\,dw}{(w^2 - 1)^{1/2} + (w^2 - n^2)^{1/2}}$$

The transformation $(w^2 - 1)^{1/2} = -iu$; $i = (-1)^{1/2}$ leads to:

$$\prod_x = -ik \int_{\gamma(u)} \left\{H_o^{(1)}\left[\rho(1 - u^2)^{1/2}\right]\right\} e^{i\sigma u}\left[F(X)\right] du$$

$$F(X) = \frac{1}{1 + \left(1 + \frac{1}{X}\right)^{1/2}} \quad ; \quad X = \frac{u^2}{n^2 - 1}$$

Note the two multivalued functions inside brackets.

II. Branch cuts. Take F(X) and use, for example, the same branch as before (see A-1). Take $(1 - u^2)^{1/2} = (1+u)^{1/2}\,(1-u)^{1/2}$ and use, for example, the same branch cut as before (see A-2).

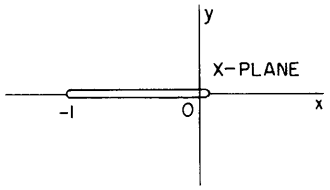

A-1

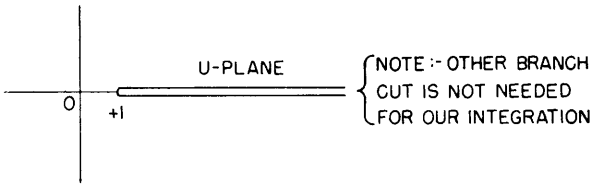

A-2

III. Distribution functions

a. Basic idea. Distribution functions are generated by a simple use of the "residue theorem" in connection with F(X) and $(1-u)^{1/2}$. The residue theorem states

$$\oint F(X)\,dX = 2\pi i \sum \text{residues in O}$$

Take F(X) first and consider the integral defined as follows:

$$\phi(x) = \frac{1}{2\pi i}\int_{-\Gamma} F(X)\,dX$$

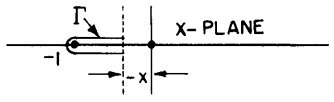

A-3

By elementary transformations, one gets

$$\phi(x) = \frac{1}{2\pi i}\int_{-1}^{-x} 2\lambda\left(1 + \frac{1}{\lambda}\right)^{1/2} d\lambda = -\frac{1}{2} + \frac{1}{\pi}\int_{0}^{x} \lambda\left(1 - \frac{1}{\lambda}\right)^{1/2} d\lambda$$

where $0 \leqslant x \leqslant 1$, which by definition is the distribution function along the cut. One obtains

$$\phi(x) = -\frac{1}{2} + \frac{1}{4\pi}\left\{\cos^{-1}(x)^{1/2} - \left[x(1-x)\right]^{1/2}(2x - 1)\right\}$$

c. A similar procedure renders the distribution function for $(1-u)^{1/2}$ as

$$\psi(u) = \frac{2}{3\pi}(u-1)^{3/2} \quad ; \quad 1 < u < \infty$$

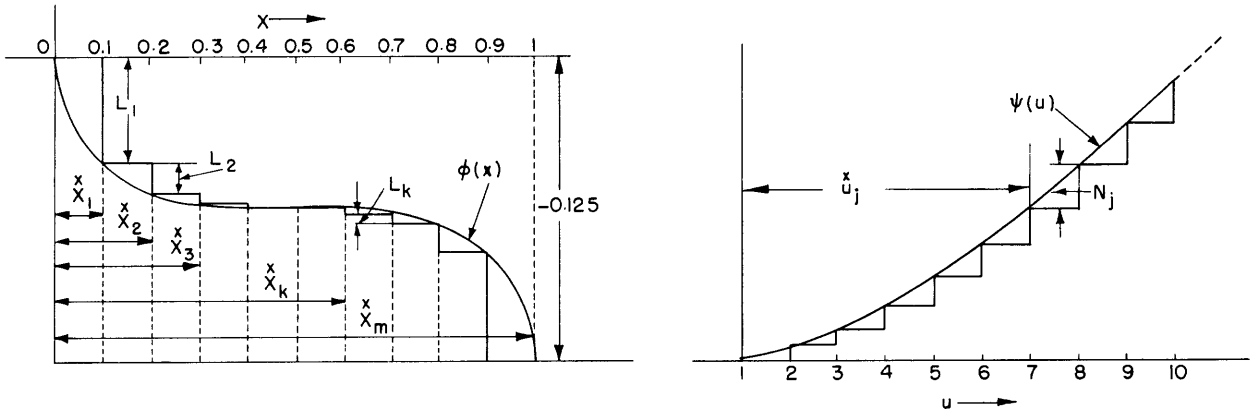

A-4

IV. Monogenic representation of the required branch of F(X) and $(1-u)^{1/2}$

$$ {}_{+}F(X) = \int_0^1 \frac{d\phi(\lambda)}{X - \lambda} \; ; \quad +(1-u)^{1/2} = \int_1^\infty \frac{d\psi(\theta)}{u - \theta} $$

They are, in this case, the "Stieltjes transforms" of $\phi(x)$ and $\psi(u)$ respectively.

V. Rational expansions. Construct the stair-like functions, as indicated in A-4. By elementary properties of Stieltjes integrals, one obtains

$$ F_m(X) = F(\infty) - \sum_{k=1}^{k=m} \frac{L_k}{X - \overset{x}{X}_k} $$

$$ G_n(u) = \sum_j \frac{N_j}{u - \overset{x}{u}_j} $$

Note that we can place the poles where it is convenient. No computation is required to find the pole positions and their residues.

VI. As before, the contribution to the integral from the branch of F(X) is

$$ \prod_{x,1} \approx \pi k i (n^2 - 1)^{1/2} \sum_{k=1}^{k=m} \frac{L_k}{(\overset{x}{X}_k)^{1/2}} H_o^{(1)} \left\{ \rho \left[1 + (n^2 - 1) \overset{x}{X}_k \right]^{1/2} \right\} $$

$$ \times \exp \left\{ -\sigma \left[(n^2 - 1) \overset{x}{X}_k \right]^{1/2} \right\} $$

VII. The contribution from the branch cut of $(1-u)^{1/2}$ is

$$\prod_{x,2} = \frac{8}{3} 2^{1/2} \rho ik \sum_j \left\{ N_j \frac{\overset{x}{u}_j (1 + \overset{x}{u}_j)^{1/2} \exp(+i\sigma \overset{x}{u}_j)}{\overset{x}{u}_j + \left[\overset{x2}{u}_j + (n^2 - 1)\right]^{1/2}} \right.$$

$$\left. \times \Lambda_{3/2} \left[2 \left(\rho N_j \sigma \left[1 + \overset{x}{u}_j \right]^{1/2} \right)^{1/2} \right] \right\}$$

References

1. E. Jahnke, F. Emde: Tables of Functions, Dover Publications, New York, 1945 (paper$1.90, cloth$3.95). Figures in Exhibit 1 were used by permission of the publishers.

2. A. Sommerfeld: Partial Differential Equations in Physics, Academic Press, New York, 1949

M. V. Cerrillo

2. Synthesis of Finite, Linear, Passive Networks for Specified Input and Output Time Response

Since the impulse response h(t) of a network is a function of time, and the network synthesis procedures available are in terms of the complex frequency

$$s = \sigma + i\omega$$

we need a system function H(s) which will represent h(t) in the s domain. The system function which has been employed is the classical Laplace transform of h(t)

$$H(s) = \int_0^\infty h(t)\, e^{-st}\, dt \qquad (1)$$

This function is included in the general Laplace-Stieltjes integral

$$H(s) = \int_0^\infty e^{-st}\, d\alpha(t) \qquad (2)$$

which also has the discontinuous representation in Dirichlet series form

$$H(s) = \sum_{n=1}^{\infty} a_n \exp(-\tau_n s) \tag{3}$$

where the a_n are the areas under the h(t) curve in the intervals between the times τ_n, as indicated in Fig. IX-19.

From the expansion

$$\exp(-\tau_n s) = 1 - (\tau_n s) + \frac{(\tau_n s)^2}{2!} - \frac{(\tau_n s)^3}{3!} + \ldots$$

which is valid for all finite s, we obtain

$$H(s) = b_0 + b_1 s + b_2 s^2 + \ldots \tag{4}$$

the power-series representation of Eq. 3.

The usefulness of these two forms of the system function is that h(t) need not be known analytically at all: Just a graph or even a time sequence at stated intervals (not necessarily equidistant) is sufficient to yield Eq. 3 or Eq. 4.

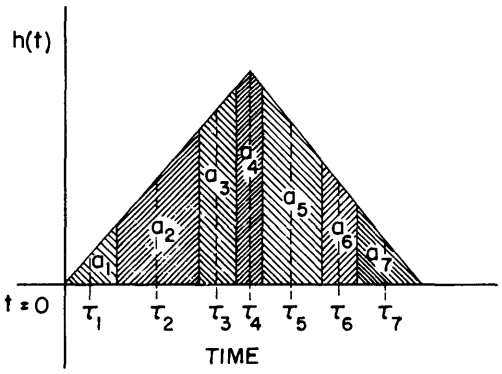

Fig. IX-19

Arbitrary impulse response denoted in terms of areas a_n and time intervals τ_n for Dirichlet series representation.

This allows us then to proceed to a very desirable development because we now can get an $H^*(s)$ which shall be a rational function. In the event that h(t) is an impulse response with a rational function for its Laplace transform, this method can give this rational function exactly. But what is more important in network engineering, even in the cases where h(t) has a transcendental function as its Laplace transform, we can still get a rational function approximation for its system function. Hence this impulse response may now be realized by a finite, linear, passive network.

Since the complete method will be described in a forthcoming technical report, it is only outlined briefly here. Essentially the procedure is to write $H^*(s)$ as

$$H^*(s) = \frac{p_0 + p_1 s + p_2 s^2 + \ldots + p_n s^n}{q_0 + q_1 s + q_2 s^2 + \ldots + q_m s^m} \tag{5}$$

where m and n can be fixed by the allowable complexity of the network, the desired tolerances in the time domain, or the initial behavior of h(t) near t = 0; and where the

coefficients $p_0, p_1, p_2, \ldots, p_n$ and $q_0, q_1, \ldots, q_m$ are to be calculated.

Let $H^*(s) = H(s)$ as given by Eq. 4. This gives two polynomials in s when we carry out the multiplication of $(q_0 + q_1 s + q_2 s^2 + \ldots + q_m s^m)$ with the right-hand side of Eq. 4. We may equate the coefficients of like powers in s in the two polynomials to yield a set of linear, simultaneous, algebraic equations, from which it is a straightforward process to solve for the unknowns.

Examples with h(t), like te^{-t}, which have H(s) that are rational functions, are worked out with complete accuracy. The computational effort is very slight and consists of only simple algebra. h(t), like $t \exp(-t^2)$, which have Laplace transforms that are transcendental, namely, $-d/ds \left[\pi^{1/2}/2 \exp(s^2/4) \operatorname{cerf}(s/2)\right]$, where

$$\operatorname{cerf}\left(\frac{s}{2}\right) = \frac{2}{\pi^{1/2}} \int_{s/2}^{\infty} e^{-x^2} dx$$

can be approximated easily with $H^*(s)$ having only a few complex poles and yet having $h^*(t)$ that are within close tolerances to h(t). The computations are of the same simple type as for the previous case.

Furthermore, this approach enables us to deal with the general problem of time-domain synthesis for arbitrary input $f_i(t)$ and output $f_o(t)$. In fact, starting from $f_i(t)$ and $f_o(t)$ as the specifications, an original procedure is now available to calculate H(s) as a rational function and thus obtain a finite, linear, passive network directly with straightforward algebraic methods.

F. Ba Hli

3. Use of the Derivative in Electrical Network Problems

Part II

In Part I (see ref. 1) it was shown that the critical points of a polynomial with simple roots coincide with the equilibrium positions in a field of force where unit masses, located in the positions of zeros of the polynomial, repel a moving unit mass according to the inverse-distance law. If p unit masses are located at a p-th order multiple root of a polynomial with multiple roots

$$f(s) = (s - s_1)^{m_1} (s - s_2)^{m_2}, \ldots, (s - s_p)^{m_p}$$

Then the equilibrium points, in addition to the multiple roots of f(s), are the zeros of Z(s)

$$Z(s) = \frac{f'(s)}{f(s)} = \sum_{j=1}^{p} \frac{m_p}{s - s_p}$$

The function $Z(s) = d/ds\left[\text{Log } f(s)\right]$ is called the logarithmic derivative of the function f(s). The logarithmic derivative of a polynomial has mathematical and physical significance. K. F. Gauss, F. Lucas, P. Montel, J. L. Walsh, M. Marden, and others who have dealt with the problem of the existing relations between the location of the critical points of a polynomial and its roots, make extensive use of the logarithmic derivative. Following this trend of thought, we may state Theorem 3 which will serve as a liaison between electrical network theory and some of the mathematical work to which we have referred.

Theorem 3: The logarithmic derivative Z(s) of a Hurwitz polynomial f(s) is a positive real function. If s is considered as the complex frequency ($s = \sigma + i\omega$), then Z(s) could present the driving-point impedance of a one terminal-pair passive network.

Proof: The lemma mentioned in Part I (ref. 1) shows that the poles and zeros of Z(s) are located in the left half-plane or on its boundary. Z(s) could be expanded as

$$Z(s) = \sum_{1}^{p} \frac{m_j}{s - s_j} , \quad m_j = \text{positive integers}$$

A root s_j either is a negative real number or it appears along with its complex conjugate in the above expansion. In the first case, $m_j/(s - s_j)$ is a positive real function representing the driving-point impedance of the parallel combination of a resistor and a capacitor. In the latter case each pair of partial fractions

$$Z_j = \frac{m_j}{s - s_j} + \frac{m_j}{s - \bar{s}_j} = \frac{m_j(2s - s_j - \bar{s}_j)}{(s - s_j)(s - \bar{s}_j)}$$

is a positive real function, with a simple RLC representation. Furthermore,

$$\text{Re } Z_j(j\omega) = \frac{-2\alpha m_j(\alpha^2 + \beta^2 + \omega^2)}{\left[(\alpha^2 + \beta^2 - \omega^2)^2 + 4\alpha^2\omega^2\right]}$$

where $s_j = \alpha + j\beta$. Re $Z_j(j\omega)$, as a function of ω, has its minimum value at $\omega = \infty$; therefore, Z(s) has an RLC Brune configuration without ideal transformers.

Corollary I: If P(s) is a Hurwitz polynomial, then

$$Z_n(s) = \frac{d^n P(s)/ds^n}{d^{n-1} P(s)/ds^{n-1}}$$

is also a positive real function; thus, $Z_n(s)$ has a network representation.

Corollary II: The logarithmic derivative of any polynomial f(s) with roots restricted to the negative real axis, represents the driving-point impedance of an RC network.

Corollary III: The logarithmic derivative of any real polynomial with roots restricted to the axis of the real frequencies represents the driving-point impedance of an LC network.

Next we establish a theorem which was first proved by Laguerre (see ref. 2, p. 200, or ref. 3, chap. 13).

Laguerre's theorem: Let P(s) be a polynomial with real coefficients and real distinct negative zeros, and let α be a positive number. Then $\alpha P(s) + sP'(s)$ is also a polynomial with real negative zeros.

Proof: In lieu of the classical proof of the theorem, we present the following proof based on electrical network considerations (see Fig. IX-20).

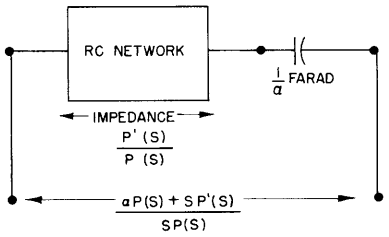

Fig. IX-20

Proof of Laguerre's theorem based on electrical analogy.

From Corollary II we see that $P'(s)/P(s)$ represents an RC network; therefore, the addition of a series capacitor of $1/\alpha$ farads to the network which represents $P'(s)/P(s)$ would not change the nature of the composite network. The over-all impedance function $\left[sP'(s) + \alpha P(s)/sP(s)\right]$ represents an RC network. This fact guarantees that poles and zeros of the latter function alternate on the negative real axis. Applying Theorem 1, we may add that if P(s) is a polynomial with distinct real negative roots, the same is true for $\alpha P^n(s) + sP^{n+1}(s)$.

a. Generation of RC polynomials

Definitions: For brevity we may call an RC polynomial any Hurwitz polynomial with distinct real negative roots. In conformity with the literature, we shall call the real functions p(s) and g(s) a "real couple," if for any real parameters μ and ν the function

$$\mu p(s) + \nu g(s)$$

has no imaginary roots (4). From this definition one concludes that the driving-point impedance of any RC or RL network is the ratio of two RC polynomials which form a real couple.

From Laguerre's theorem one may conclude that if Eq. 1 is an RC polynomial,

$$f_1(s) = \sum_0^n a_n s^n \tag{1}$$

The same is true for Eq. 2

$$f_2(s) = \sum_0^n a_n(a+n)s^n \tag{2}$$

a being an arbitrary positive quantity. Iteration of Eq. 2 leads to the fact that Eq. 3 is also an RC polynomial, provided Q(n) is an RC polynomial in n (see ref. 3)

$$f_3(s) = \sum_0^n a_n Q(n) s^n \tag{3}$$

Further extension shows that if Eq. 1 is an RC polynomial and a and g are positive constants, then

$$f_4(s) = \sum_0^n \frac{(n+a)\,(n+a+1)\,\ldots\,(n+a+q)}{q^{n+a}\cdot q!} a_n s^n \tag{4}$$

is also an RC polynomial.

These formulas give an idea how one may go about generating RC polynomials from a given RC polynomial. The physical significance behind the mathematics of the generation of RC polynomials seems to be the fact that the composition and series-parallel combinations of RC networks must lead to an RC network.

It is also possible to generalize the above considerations in order to obtain certain transcendental functions. In fact, if q becomes very large in Eq. 4, then

$$f_5(s) = \sum_0^n \frac{a_n s^n}{\Gamma(a+n)} \tag{5}$$

which is also an RC polynomial. The work of Laguerre, Tschebotrarŏw (4), Polya (5), N. Obrechkoff (6), and others in this field is worth investigating with the idea of RC network representation of some transcendental functions.

A systematic generalization of the method of generation of RC polynomials to real couples will make it possible to generate the latter couples. For example, as it was mentioned before, if P(s) is an RC polynomial, then P(s) and aP(s) + sP'(s) must form a real couple. Similiar considerations lead to the following more general statement.

Theorem 4: If

$$Z(s) = \frac{a_0 + a_1 s + \ldots + a_n s^n}{b_0 + b_1 s + \ldots + b_n s^n}$$

represents the driving-point impedance of a two-element type, one terminal-pair

dissipative network, and P(s) is an RC polynomial, then

$$Z_k(s) = \frac{a_0 P + a_1 P' + \ldots + a_n P^n}{b_0 P + b_1 P' + \ldots + b_n P^n}$$

will also represent the driving-point impedance of a two-element type one terminal-pair dissipative network.

Further extension of the use of the derivative in the network problems is being investigated. In a way, it seems possible to connect the classical network theory to the theory of differential equations. In fact, we have already considered the connection between some RC polynomials and driving-point impedances with the famous differential equations of physics. The details need further time to be worked out.

F. M. Reza

References

1. Quarterly Progress Report, Research Laboratory of Electronics, M.I.T. April 15, 1953, pp. 57-61
2. E. -N. Laguerre: Oeuvre, Tome 1, Libr. Gauthier-Villars, Paris, 1898
3. G. Valiron: Théorie des Fonctions, Masson et Cie, Éditeurs, Paris, 1942, chap. 13
4. N. Tschebotrarëw: On Entire Functions with Real Interlacing Roots, Comptes Rendus (Doklady) de l'Académie des Sciences de U.R.S.S. 35, 195-197, 1942
5. G. Polya: Rendiconti Circ. Mat., Palermo, 36, 279-295, 1913
6. N. Obrechkoff: Sur les fonctions entières limites de polynômes dont les zeros sont réel et entrelacés, Mathematicheskii Sbornik 9, 421-427, 1941

4. Conversion of a Brune Cycle with an Ideal Transformer into a Cycle without an Ideal Transformer

a. Introduction

O. Brune (1) has proved that any rational "positive real" function represents a one terminal-pair network configuration containing a finite number of linear passive elements. Brune suggested the ladder synthesis for positive real functions, but this is generally confronted by mutual couplings, which are not desirable from a practical standpoint. Thus there has always been a great desire to eliminate ideal transformers from the picture. As steps towards this goal, H. W. Bode suggests resistance padding, and E. A. Guillemin (2) often uses some practical methods for eliminating the ideal transformer in special cases. The existence proof along with a synthesis procedure without an ideal transformer was first given by R. Bott and R. J. Duffin (3).

The object of this report is to outline some results which have been found by the author:

> By the continuation of the Brune synthesis procedure we have arrived at Bott and Duffin's result. This provides an alternative proof to that of Bott and Duffin for the existence of a network configuration without an ideal transformer for any positive real function.
>
> Our method of approach suggests a more unified synthesis procedure: Follow the Brune synthesis procedure. If a Brune cycle with an ideal transformer is confronted, convert that cycle into a cycle without a transformer. Numerical values of the elements of the latter cycle are found in terms of elements of the corresponding Brune cycle.

b. Existence proof

In the Brune synthesis of a driving-point impedance Z(s), when Re Z(jω) has a finite minimum along the axis of real frequencies, one is confronted with an ideal transformer. Let Z(s) be such a function, whose minimum real part has already been removed. It is known (1, 4) that the removal of elements L_1, L_2, L_3 (L_3 assumed negative), and c as shown in Fig. IX-21 will lead to a positive real function z which may or may not contain an ideal tranformer in its Brune configuration. From Fig. IX-21 it is seen that

$$\frac{1}{Z - L_1 s} = \frac{cs}{cL_2 s^2 + 1} + \frac{1}{L_3 s + z} \tag{1}$$

$$Z_1(s) = Z - L_1 s = \frac{(L_3 s + z)(cL_2 s^2 + 1)}{\left[c(L_3 + L_2)s^2 + 1\right] + csz}$$

It is known to those using the Brune synthesis that the function $(Z - L_1 s)$ has only one positive real zero, a fact which necessitates an ideal transformer in this synthesis. For the sake of future reference we may conveniently state this fact in the following theorem.

Theorem: Let Z(s) be a positive real function and A a positive constant. Then Z(s) - As = 0 cannot have more than one zero in the right half-plane.

Proof of this theorem was first given by Brune (ref. 1, Theorem VI, Corollary I). An independent proof has also been established by the author. (This proof will not be presented in this report.)

If the positive real root which enters Eq. 1 is denoted as k, then

$$Z(k) - L_1 k = 0 \tag{2}$$

$$z(k) + L_3 k = 0 \tag{3}$$

In an attempt to avoid the obstacle of the ideal transformer it seems natural at first to attempt the Brune synthesis of the reciprocal function on the admittance basis (see ref. 4, page 268).

$$\frac{1}{Z(s)} - As$$

where A is a positive constant.

Based on the above theorem, it could be shown that if Z(s) satisfies the conditions outlined above, then

$$Z_2 = \frac{1}{Z} - As$$

has all its poles and zeros in the left half-plane, except for one positive real zero. One may select A so that the positive real root Z_2 coincides with that of Z_1. In that case,

$$\frac{1}{Z(k)} - Ak = 0, \quad A = \frac{1}{L_1 k^2} \tag{4}$$

Now consider the function

$$\frac{Z - L_1 s}{\frac{1}{Z} - \frac{s}{k^2 L_1}} = \frac{Z - L_1 s}{k^2 L_1 - sZ} \cdot k^2 L_1 Z$$

and let

$$Z_3(s) = k\left(\frac{Z - L_1 s}{k^2 L_1 - sZ}\right) \tag{5}$$

It can be shown that Z_3 is a positive real function: its poles and zeros are in the left half-plane, the difference of the degree of its numerator and denominator is not more than one, and Re $Z_3(j\omega) \geq 0$, as shown below

$$\text{Re } Z_3(j\omega) = k \frac{L_1 U(k^2 + \omega^2)}{(k^2 L_1 + \omega V)^2 + \omega^2 U^2} \tag{6}$$

where

$$Z(j\omega) = U + jV$$

The network configuration of Fig. IX-22 is an immediate consequence of Eqs. 5 and 7.

$$Z = \frac{1}{\frac{Z_3}{L_1 k} + \frac{1}{L_1 s}} + \frac{1}{\frac{s}{L_1 k^2} + \frac{1}{kL_1 Z_3}} \tag{7}$$

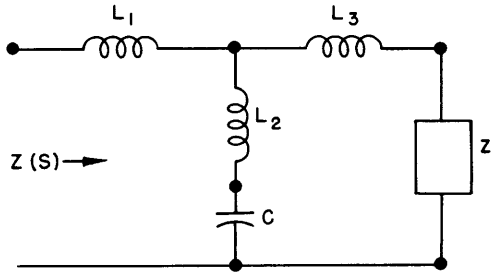

Fig. IX-21
A Brune cycle, $L_3 < 0$.

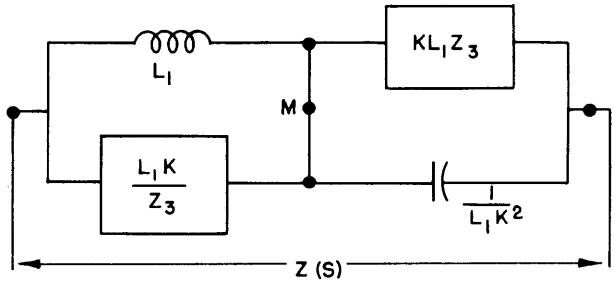

Fig. IX-22
Equivalent of Fig. IX-21 using Eq. 7.

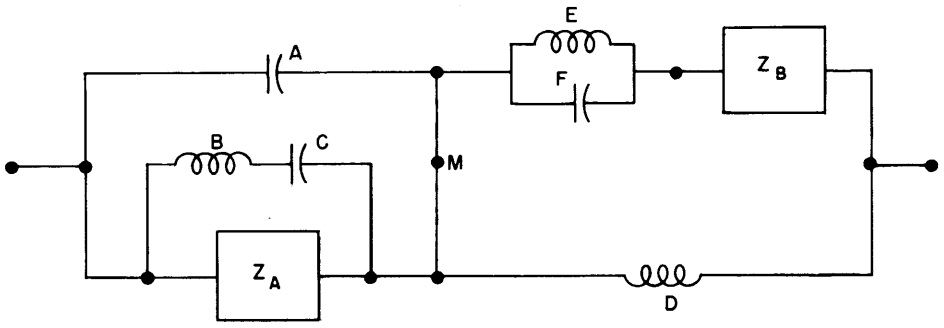

Fig. IX-23
Equivalent for the Brune cycle of Fig. IX-21. For the values of A, B, C, D, E, F, Z_A, and Z_B refer to the summary of the procedure in the text.

c. Synthesis of Z_3

Using formulas 1 and 5, we will find

$$\frac{1}{Z_3} = \frac{L_1(k^2 - s^2)\left[csz + c(L_2 + L_3)s^2 + 1\right] - s(L_3 s + z)(L_2 cs^2 + 1)}{k(L_3 s + z)(cL_2 s^2 + 1)} \tag{8}$$

which suggests that a pair of poles of $1/Z_3$ on the axis of imaginaries could be removed. To find the values of elements corresponding to this pair of poles, one can proceed by finding the proper residues:

$$\text{residue of } \left[\frac{1}{Z_3}\right] \text{ at } \frac{\pm j}{(L_2 c)^{1/2}} = \frac{L_1(k^2 L_2 c + 1)}{2kL_2^2 c} \tag{9}$$

Let the corresponding elements be L_ν and c_ν. Then

$$L_\nu = \frac{L_1(k^2 L_2 c + 1)}{kL_2}$$

$$c_\nu = \frac{kL_2^2 c}{L_1(k^2 L_2 c + 1)} \tag{10}$$

The network of Fig. IX-22 with proper impedance levels for Z_3 will lead, along with the results outlined in Eqs. 8 and 10, to the final conversion cycle such as that shown in Fig. IX-23.

In the particular case of a quadratic rational fraction, one obtains the equivalent network, without an ideal transformer, by letting z = r in Fig. IX-21, and

$$k = \frac{-r}{L_3}, \qquad Z_A = r, \qquad \text{and} \qquad Z_B = \frac{r(L_1 + L_2)}{L_2 + L_3} \tag{11}$$

in Fig. IX-23.

It is important to note that the structure of Figs. IX-23 and IX-22 represent a balanced bridge. In fact

$$L_1 s \times \frac{L_1 k^2}{s} = \frac{L_1 k}{Z_3} \times kL_1 Z_3 = k^2 L_1^2 \tag{12}$$

which shows that the opening of the node M will not destroy the balance of the bridge. This reduces Fig. IX-22 to one loop in conformity with reference 5.

This method may be summarized as follows:

1. Proceed with the Brune synthesis in general. If confronted with an ideal transformer, finish the Brune cycle and find L_1, L_2, L_3, c and k.
2. Draw Fig. IX-23 and compute the proper values of A, B, C, D, E, F, Z_3, Z_A, and Z_B as shown below.

$$A = \frac{1}{L_1 k^2} \qquad D = L_1$$

$$B = \frac{k^2 L_2^2 c}{k^2 L_2 c + 1} \qquad E = \frac{L_1^2(k^2 L_2 c + 1)}{L_2}$$

$$C = \frac{k^2 L_2 c + 1}{k^2 L_2} \qquad F = \frac{L_2^2 c}{L_1^2(k^2 L_2 c + 1)}$$

$$\frac{1}{Z_3} = \frac{L_1 k^2 - sZ}{k(Z - L_1 s)} = \frac{L_1(k^2 - s^2)\left[csz + c(L_2 + L_3)s^2 + 1\right]}{k(L_3 s + z)(cL_2 s^2 + 1)} - \frac{s}{k}$$

$$\frac{1}{Z_A} = \frac{1}{kL_1 Z_3} - \frac{(k^2 L_2 c + 1)s}{k^2 L_2(cL_2 s^2 + 1)} \qquad Z_B = \frac{L_1 k}{Z_3} - \frac{L_1^2(k^2 L_2 c + 1)}{L_2(cL_2 s^2 + 1)}$$

3. Follow the Brune procedure on Z_A and Z_B. If the Brune synthesis of Z_A or Z_B again introduces ideal transformers, proceed again as in step 2.

F. M. Reza

References

1. O. Brune: J. Math. Phys. 10, 191, 1931
2. E. A. Guillemin: Unpublished material for courses on Advanced Network Theory, Department of Electrical Engineering, M.I.T.
3. R. Bott, R. J. Duffin: J. Appl. Phys. 20, 816, 1949
4. E. A. Guillemin: A Summary of Modern Methods of Network Synthesis, Advances in Electronics, Vol. 3, Academic Press, New York, 1951, p. 268
5. F. M. Reza: Quarterly Progress Report, Research Laboratory of Electronics, M.I.T. Jan. 15, 1953

G. COMMUNICATIONS BIOPHYSICS

Prof. W. A. Rosenblith
K. Putter
R. M. Brown

1. Anechoic Chamber

Within the last two months R. Brown has reworked the electrical shielding of the anechoic chamber and has overcome most of the problems that had arisen.

Potentials from the auditory cortex of a cat and from the auditory nerve of a monkey have been successfully recorded. The former experiment was done in cooperation with Dr. Mary A. B. Brazier, Massachusetts General Hospital; the latter, in cooperation with Dr. K. Pribram, the Institute of Living, Hartford, and Dr. B. Rosner, Yale University.

W. A. Rosenblith, K. Putter, R. M. Brown

2. Instrumentation

Final tests on the preliminary model of the time-gated amplitude quantizer indicated that some refinement of the circuit design will allow extension of the original specifications. Accordingly, the unit has been redesigned to handle responses to stimulus repetition rates from approximately 10 per second to 1 every 10 seconds. Some effort has also been made to increase the number of levels of quantization to 40. The final model, incorporating the design changes, is in the process of construction.

K. Putter

3. Electrical Responses to Clicks Recorded from Eighth-Nerve Locations in Monkey*

Acoustic clicks evoke changes in potentials that can be recorded by wire electrodes at the eighth nerve in the cerebellopontine angle. These potentials change in amplitude and latency with stimulus intensity. The earliest deflections occur, for clicks approximately 60 db above threshold, 1.75 msec after the acoustic stimulus impinges upon the eardrum. In the presence of a simultaneous masking noise, these neural potentials are reduced in amplitude: as the intensity of the masking noise increases, the neural response to a click decreases in size. If pairs of clicks are presented, the amplitude of the response to the second of the pairs of clicks is a function of the intensity of the

*Abstract of a paper presented to the meetings of the Federation of American Societies for Experimental Biology, Chicago, April 6-10, 1953.

first click and of the time interval between the clicks (for time separations up to more than 100 msec). Cutting the nerve abolishes the later components of the response but leaves intact the interaction between the remaining responses to pairs of clicks.

W. A. Rosenblith

(IX. COMMUNICATION RESEARCH)

H. NEUROPHYSIOLOGY*

W. S. McCulloch
B. Howland
J. Y. Lettvin
W. H. Pitts
P. D. Wall

During the past term we finished five major experiments:

We investigated with Dr. V. Amassian from the University of Washington the action of strychnine in the spinal cord. In 1950, we noted that the drug seemed to increase the membrane potential of the afferent fibres, certainly intramedullarly and probably in the proximal portions of the root. A result of such a rise in membrane potential would be an increase in threshold. We inserted a microelectrode this time into the dorsal portions of the ventral horn and used it to stimulate, getting the Renshaw picture of the direct and relayed volleys in the ventral root. Under strychnine the relayed volley was greatly enhanced and the direct volley was reduced, showing that the ventral horn cells had suffered an increase in threshold. We are therefore more sure of our interpretation of strychnine action at a relay as being the enhancing of the input signal. One of the curious subsidiary observations in this experiment was that the reduction of muscle tone, say by curare, abolishes the monosynaptic arc.

We examined the actual properties of our platinum microelectrodes in tissue and discovered that the resistance and the reactance are proportional to $f^{-0.95}$; R = 10 megohms, X_c = 100 megohms at 10 cps. The resistance of tissue around the tip is about 150,000 ohms in grey matter and about 500,000 ohms in white, which compares with a resistance of 15,000 ohms in normal saline. Above 1 kc, it is the resistance of the medium that is the major component of the total electrode resistance.

We have made a map of the inhibitory action of a conditioning dorsal root volley on the test volley in an adjacent dorsal root at 30 msec after conditioning stimulus. The results are too lengthy to be presented here, but may be summarized thus: At this interval there is a major source in the dorsal columns and a set of distributed sinks in the grey matter; both are significantly removed from the boundary. This sort of inhibition seems to be a dimunition in the dorsum of the normal sources and sinks invading the grey up to 1.5 msec after the test stimulus. We are reasonably sure that this supports the idea that one form of inhibition consists of attenuating the input signal.

The distribution of sources and sinks at 30 msec after the conditioning stimulus suggested that the dorsal root long negative potential (DR 5) was in fact not to be attributed to internuncial activity. We anaesthetized a cat's spinal cord to the point where, with a microelectrode, no cellular activity could be observed anywhere in response to

---

*The work reported in this section has been supported in part by the Bell Telephone Laboratories, Incorporated, and by a separate contract with the Office of Naval Research.

dorsal root stimulation and were still able to recover an unchanged sequence of the dorsal root potential somewhat diminished in amplitude. This experiment effectively disproves the hypothesis of internuncial origin of DR 5 and instead confirms the suggestion made by Dr. Mary Brazier's group (Massachusetts General Hospital) that it is the electrotonic spread of the negative after-potential of the unmyelinated terminal arbor.

We did some preliminary mapping of the effects of stimulation by a microelectrode in different parts of the cord one segment away from the stimulated segment. One consequence was that a long and late inhibition of spinal reflexes could be obtained from lateral white matter, and an early short inhibition produced from the ventromedial white; the latter observation tends to confirm our earlier studies on bulbar reticular inhibitory pathways.